Journal of Cerebral Blood Flow & Metabolism (2012) 32, 1800–1809
© 2012 ISCBFM All rights reserved 0271-678X/12 $32.00
www.jcbfm.com

Dynamic functional cerebral blood volume responses to normobaric hyperoxia in acute ischemic stroke

Ona Wu[1], Jie Lu[2], Joseph B Mandeville[1], Yoshihiro Murata[2], Yasu Egi[2], Guangping Dai[1], John J Marota[3], Izzuddin Diwan[1], Rick M Dijkhuizen[4], Kenneth K Kwong[1], Eng H Lo[2] and Aneesh B Singhal[5]

[1]*Athinoula A. Martinos Center for Biomedical Imaging, Massachusetts General Hospital, Charlestown, Massachusetts, USA;* [2]*Neuroprotection Laboratory, Department of Radiology, Massachusetts General Hospital, Charlestown, Massachusetts, USA;* [3]*Department of Anesthesiology, Massachusetts General Hospital, Boston, Massachusetts, USA;* [4]*Biomedical MR Imaging and Spectroscopy Group, Image Sciences Institute, University Medical Center Utrecht, Utrecht, The Netherlands;* [5]*Department of Neurology, Massachusetts General Hospital, Boston, Massachusetts, USA*

Studies suggest that neuroprotective effects of normobaric oxygen (NBO) therapy in acute stroke are partly mediated by hemodynamic alterations. We investigated cerebral hemodynamic effects of repeated NBO exposures. Serial magnetic resonance imaging (MRI) was performed in Wistar rats subjected to focal ischemic stroke. Normobaric oxygen-induced functional cerebral blood volume (fCBV) responses were analyzed. All rats had diffusion-weighted MRI (DWI) lesions within larger perfusion deficits, with DWI lesion expansion after 3 hours. Functional cerebral blood volume responses to NBO were spatially and temporally heterogeneous. Contralateral healthy tissue responded consistently with vasoconstriction that increased with time. No significant responses were evident in the acute DWI lesion. In hypoperfused regions surrounding the acute DWI lesion, tissue that remained viable until the end of the experiment showed relative preservation of mean fCBV at early time points, with some rats showing increased fCBV (vasodilation); however, these regions later exhibited significantly decreased fCBV (vasoconstriction). Tissue that became DWI abnormal by study-end initially showed marginal fCBV changes that later became moderate fCBV reductions. Our results suggest that a reverse-steal hemodynamic effect may occur in peripheral ischemic zones during NBO treatment of focal stroke. In addition, CBV responses to NBO challenge may have potential as an imaging marker to distinguish ischemic core from salvageable tissues.
Journal of Cerebral Blood Flow & Metabolism (2012) **32,** 1800–1809; doi:10.1038/jcbfm.2012.87; published online 27 June 2012

Keywords: acute stroke; brain imaging; BOLD contrast; cerebral hemodynamics; focal ischemia

Introduction

Studies in experimental stroke models and acute human stroke patients indicate that normobaric oxygen therapy (NBO) may be a potent neuroprotectant (Henninger *et al*, 2007; Liu *et al*, 2006; Singhal *et al*, 2002, 2005). The neuroprotective effects were most evident during NBO therapy and to some extent immediately post-therapy. Tissue originally abnormal on magnetic resonance imaging (MRI)-based apparent diffusion coefficient (ADC) maps, a measure of cytotoxic edema and cellular damage, tended to recover (i.e., reverse acute ADC reductions) more often in animals and patients given NBO therapy than in control groups. Lactate levels were also shown to decrease during NBO but increased post-NBO (Singhal *et al*, 2007). These results suggest that NBO therapy may be useful for extending the therapeutic time window for stroke by slowing down the process of ischemic cell death.

NBO does not significantly increase plasma concentration of dissolved oxygen, however, it is believed to afford neuroprotection via multiple

Correspondence: Dr O Wu, Athinoula A. Martinos Center for Biomedical Imaging, 149 13th Street CNY 2301, Charlestown, MA 02129, USA.
E-mail: ona@nmr.mgh.harvard.edu
This study was supported in part by grants from the US National Institutes of Health (R01NS051412, R01NS59775, P50NS051343, and NCRR grants R03 EB008134 and P41RR14075), and the Royal Netherlands Academy of Arts and Sciences.
Received 20 January 2012; revised 5 May 2012; accepted 7 May 2012; published online 27 June 2012

indirect mechanisms (Singhal, 2007). Normobaric oxygen is known to induce vasoconstriction systemically and in the healthy brain; however, the hemodynamic effects of NBO appear to be different in the setting of acute ischemia (Lodato, 1989; Nakajima *et al*, 1983). Results of our earlier studies using dynamic susceptibility-contrast perfusion-weighted imaging (PWI) to measure relative cerebral blood volume (CBV), showed relative CBV preservation in ischemic brain tissue of rats and human subjects treated with NBO as compared with those receiving room air (RA; Singhal *et al*, 2002, 2005). Rodent studies using laser speckle flowmetry (Shin *et al*, 2007) showed that post-ischemic NBO caused an immediate increase in oxyhemoglobin concentration in the ischemic core, and improved cerebral blood flow (CBF) in the ipsilesional cortex. A study using electron paramagnetic resonance oximetry to measure interstitial oxygen tension (pO_2; Liu *et al*, 2006) found that NBO significantly increased pO_2 in the penumbra but not in the core. These results suggest that NBO's hemodynamic effects partly result from the shunting of blood from healthy to perfusion-deprived but still viable 'penumbral' brain tissue (i.e., reverse-steal or 'Robin Hood' effect; Lassen and Palvolgyi (1968)), possibly due to improved neurovascular coupling (Dirnagl, 1997; Shin *et al*, 2006) in penumbral regions.

In this study, we investigated NBO-induced spatial and temporal changes in functional CBV (fCBV) measured with MRI using superparamagnetic intravascular contrast agents with long blood half-life. Functional CBV allows us to interrogate the spatiotemporal response to NBO with greater temporal resolution than single time point PWI-based CBV measurements from bolus tracking can provide. Further, functional CBV mapping allows for comparison of simultaneous changes in both ipsilateral and contralateral tissue with respect to baseline status.

Materials and methods

Animal Preparation

All procedures were approved by our institution's animal care and use committee, Subcommittee on Research Animal Care (SRAC), which serves as the Institutional Animal Care and Use Committee for Massachusetts General Hospital. The SRAC satisfies the requirements of both the Public Health Service and the United States Department of Agriculture (USDA). Unilateral stroke was induced in adult male Wistar rats ($n = 10$; 290 to 335 *g*; Charles River Laboratories, MA, USA) by permanent occlusion of the right middle cerebral artery (MCAO) using a standard intraluminal filament technique (Longa *et al*, 1989) under isofluorane anesthesia with mechanical ventilation. Arterial blood gas (ABG) samples (pH, pCO_2, pO_2) and mean arterial blood pressure (MABP) were obtained from a femoral artery catheter and monitored throughout the experiment. Immediately after stroke induction, animals were positioned in an MRI scanner using an MRI-compatible rat stereotaxic headset with ear- and tooth-bars and mechanically ventilated under isofluorane anesthesia (1.1% to 1.5%).

Magnetic Resonance Imaging

MRI experiments were performed on a horizontal bore 9.4 Tesla Bruker Biospec Imager (Bruker Biospin, Billerica, MA, USA), equipped with a home-built rat head surface radiofrequency (RF) transmit and receiver coil with a diameter of ~30 mm. Diffusion-weighted MRI (DWI) was acquired using a diffusion tensor MRI sequence with field of view of $25 \times 25\,mm^2$, 64×64 imaging matrix, nine contiguous slices (1 mm per slice) and repetition time (TR)/echo time (TE) = 10,000/38 ms with diffusion gradients applied in six non-collinear directions with *b*-value = $997\,s/mm^2$ and one with *b*-value = $0\,s/mm^2$. Arterial spin label (ASL) perfusion-weighted measurements were made using the two-coil continuous arterial spin-labeling method with three contiguous 1 mm slices with TR/TE = 3,700/13 ms involving paired acquisitions with and without arterial spin tagging repeated 16 times. With the same slices and position as the DWI, conventional gradient echo (GRE) images were acquired with TR/TE = 300/5 ms, flip angle = 35°. Conventional GRE was used instead of echo-planar imaging-based GRE in order to use a short TE to reduce susceptibility artifact, improve signal-to-noise ratio and reduce blood oxygenation level-dependent (BOLD) signal contamination, which can obscure the detection of changes in CBV (Mandeville *et al*, 2004).

Experimental Protocol

The experimental protocol is shown in Figure 1. Baseline DWI, ASL, and GRE were obtained before injection of monocrystalline iron oxide nanocolloid (MION, 40 mg/kg). Baseline DWI consisted of two averages (scan time 2 minutes and 20 seconds). During the baseline BOLD GRE acquisition, hyperoxia-challenge was given using a block paradigm of 3 minutes RA (21% FiO_2), 4 minutes NBO (100% FiO2), and 4 minutes RA. This NBO challenge was performed before MION administration to check the ventilation lines and oxygen delivery by measuring NBO-induced signal changes in the sagittal sinus. The baseline BOLD GRE data also serve as the pre-MION data set needed for fCBV calculation. After MION injection at ~60 minutes post-MCAO, GRE data were acquired continously for 22 minutes using the paradigm of 2 minutes RA, 10 minutes NBO, and 10 minutes RA to measure oxygen-induced changes. Then, DWI was acquired using three averages to increase the signal-to-noise ratio (scan time 3 minutes and 30 seconds). The GRE/DWI set of acquisitions was repeated in 30-minute blocks for up to 4 hours in order to evaluate for ADC lesion expansion and spatial/temporal changes in CBV. Paired ABG measurements were obtained during the RA and NBO exposures (i.e., 2 measurements) at two time points: at ~1.5 hours and at ~3 hours post-MCAO. Arterial blood gas was also measured in RA conditions pre-MRI (baseline) and at the end of the MRI experiment (final). MABP were averaged over a 2-minutes period before ABG draws.

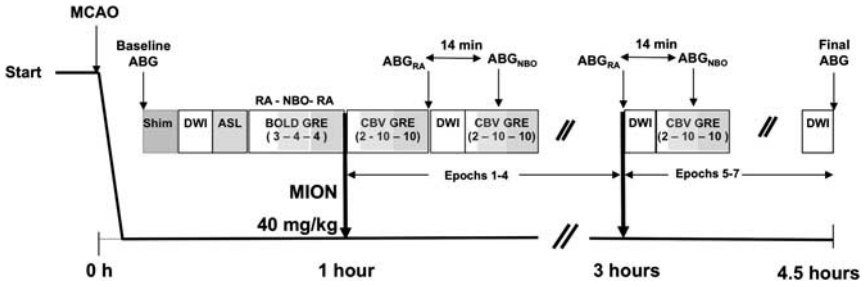

Figure 1 Imaging protocol schema. For the oxygen challenge sequences, the values in parenthesis represent duration in minutes of room air (RA), normobaric oxygen (NBO), and RA exposure. ABG, arterial blood gas; ASL, arterial spin label; BOLD, blood oxygenation level-dependent signal; CBV, cerebral blood volume; DWI, diffusion-weighted imaging; GRE, gradient echo imaging; MCAO, middle cerebral artery occlusion; MION, monocrystalline iron oxide nanocolloid.

Image Analysis

ADC maps were calculated from the DWI data from the slope of the linear regression fit of the log of the DWIs and $b = 0\,s/mm^2$ data sets (Sorensen *et al*, 1999). All ASL and GRE images were motion corrected (AFNI; Cox, 1996). Unless otherwise stated, all of the following imaging analyses were performed using JIP fMRI Analysis Toolkit, software developed in-house (http://www.nitrc.org/projects/jip/). ASL data were first spatially smoothed with 0.75 full-width half-maximum two-dimensional filter. Differences between tagged and untagged images were calculated and averaged across time to produce an index of CBF (CBF_i). DWI, CBF_i, and GRE maps were co-registered to the Paxinos–Watson Rat Brain atlas (dimension $0.25 \times 0.25 \times 1\,mm^3$). After co-registration, all data sets included slices that corresponded to bregma $+0.7$ mm to bregma -1.3 mm, in 1 mm increments. Analyses were restricted to brain parenchyma within these slices.

MRI data for each rat were automatically segmented into the following three stroke-affected regions of interest (ROIs): (1) the initial ADC lesion, (2) the initial ASL perfusion deficit, and (3) the last ADC lesion acquired at the end of the experiment. Lesions on ADC maps were defined as tissue with ADC values $\leq 78\%$ of mean value measured in the contralesional hemisphere, a threshold that had been previously shown to correspond with tissue exhibiting injury on triphenyltetrazolium-chloride staining (Miyabe *et al*, 1996). Index of CBF lesions were defined as tissue with values $\leqslant 50\%$ of the mean value measured in the contralesional hemisphere, consistent with a previous study, which used a threshold of 31 mL/100 g/min (Hoehn-Berlage *et al*, 1995), assuming normal contralateral flow is 60 mL/100 g/min. All thresholded lesion masks were then post-processed using a median-filter and 3D-connected component analysis (Matlab 7.4, Mathworks, Natick, MA, USA) to remove false positives, defined as lesion clusters $< 1\,mm^3$. Each of the three ROIs was averaged across animals to investigate the frequency of infarction as a function of location across animals. 'Saved' tissue was defined as the difference between CBF_i and the last ADC lesion and 'Growth' tissue was defined as the difference between the last and initial ADC ROIs. The ROIs were mirrored to provide contralesional control data.

The registered GRE data were spatially smoothed (0.75 mm full-width half-maximum 3D filter) and fCBV maps calculated (Mandeville *et al*, 1998). For the pre-MION images used in the fCBV determination, the 3 minutes baseline data set before NBO exposure in the BOLD GRE data set were used. For the baseline value in each fCBV calculation, the 2 minutes baseline was used in the CBV GRE block. Functional CBV responses to the oxygen challenges were analyzed using generalized linear model analysis (GLM) (Liu *et al*, 2007; Worsley *et al*, 2002) on data sets concatenated across all animals using MABP and oxygen challenges as regressors. MABP was included as a regressor because previous studies have shown increases in MABP in response to hyperoxia (Robertson *et al*, 2011), and this increase can influence the CBV signal change particularly if autoregulation is impaired. MABP data were decimated to match the sampling rate of the imaging study. Each oxygen challenge was treated as separate epochs binned as follows: 0 to 90 (Epoch 1), 91 to 120 (Epoch 2), 121 to 150 (Epoch 3), 151 to 180 (Epoch 4), 181 to 210 (Epoch 5), 211 to 240 (Epoch 6), and 241 to 270 (Epoch 7) minutes post-MCAO. We examined changes within fCBV at Epoch 1, combined Epochs 5 to 7, and differences in response between Epochs 1 to 4 (early) and 5 to 7 (late). Functional CBV was fit using an impulse response function of the form Ad/Td*exp(−t/Td) + Af/Tf * exp(−t/Tf) + As/Ts*exp(−t/Ts), with $Ad = -0.09$, $Af = 0.33$, $As = 0.67$, $Td = 0.5$ seconds, $Tf = 2.5$ seconds, $Ts = 13.5$ seconds. Temporal data are shown after removal of baseline drift that was fit in the GLM using a second-order polynomial. Regions of interests were selected on functional maps using fixed-effects analysis with a P value threshold of 0.0001 and minimum cluster size of 5, resulting in the probability of false-positive clusters to be ≤ 0.01 (3dClustSim, AFNI; Cox 1996).

Statistical Analysis

Arterial blood gas measurements and lesion volumes were compared using one-way repeated measures analysis of variance (ANOVA) with *post-hoc* Student Newman–Keuls testing (Kaledagraph 4.1, Synergy Software, Reading, PA, USA) at ~ 1.5 hours and 3 hours post-MCAO.

Baseline-corrected fCBV responses to NBO in Core, Growth, and Saved ROIs were averaged across each Epoch and compared (ANOVA followed by *post-hoc* Student Newman–Keuls test) to investigate spatial differences in response to NBO. Functional CBV changes across Epochs in each ROI were also compared (one-way ANOVA) to determine whether reactivity to NBO changed over time.

Results

Of the 10 animals we excluded two animals, one due to failed arterial occlusion (no evident perfusion lesion) and the other because of extensive imaging artifacts. All remaining eight animals contributed data for Epochs 1 and 2. One animal died ~2 hours after MCAO before the final ABG measurement could be obtained. A second animal became hemodynamically unstable after Epoch 4, at ~3 hours and the MRI study was aborted. Epochs 5 and 6 consisted of five animals each, one Epoch lost in a rat due to motion.

Table 1 shows the differences in ABG measurements and MABP at baseline, 1.5 hours, 3 hours, and final time points. Baseline and final ABG measurements were in the normal range. As expected, pO_2 levels significantly increased during hyperoxia at 1.5 hours and 3 hours compared with baseline, RA, and final levels. MABP were also found to be significantly higher during hyperoxia compared with RA at both 1.5 hours and 3 hours. Baseline MABP values were significantly higher than RA and final time points, most likely because the blood pressure lowering effects of anesthesia increased with adjustments during the MRI acquisition. PCO_2 levels, which can influence CBV, did not show significant change.

The initial ADC and the last ADC maps were acquired at 40 ± 6 minutes and 225 ± 57 minutes post-MCAO, respectively. Figure 2 shows the average incidence of lesions identified across all the animals. Using one-way ANOVA, initial ADC, CBF_i, and last ADC lesion volumes were found to be significantly different from one another ($P < 0.001$). The CBF_i (90.3 ± 5.8 mm^3) and the last ADC (56.9 ± 21.8 mm^3) lesion volumes were significantly larger ($P < 0.001$) than the initial ADC (23 ± 14 mm^3) lesions. The CBF_i lesions were also significantly larger than the ADC lesion volumes measured at the last time point ($P < 0.001$). Figure 3 shows the evolution of the ADC lesion volumes over time for each rat. Initial ADC lesions were primarily restricted to include the striatum, globus pallidus, and the hypothalamus, whereas perfusion deficits encompassed the entire right MCA territory. By the last ADC acquisition, lesions had expanded and included the somatosensory cortex.

Functional CBV results demonstrated spatially and temporally heterogenous CBV responses to NBO (Figure 4). Representative acute CBF and ADC maps and last ADC maps and automatically segmented regions are also shown (Figure 4A). The Core region showed no change in fCBV responses to NBO challenge (Figure 4B). This is to be expected as there is no or very low flow to this region. Heterogeneity in fCBV response was apparent even within the ipsilesional 'mismatch' regions consisting of Growth

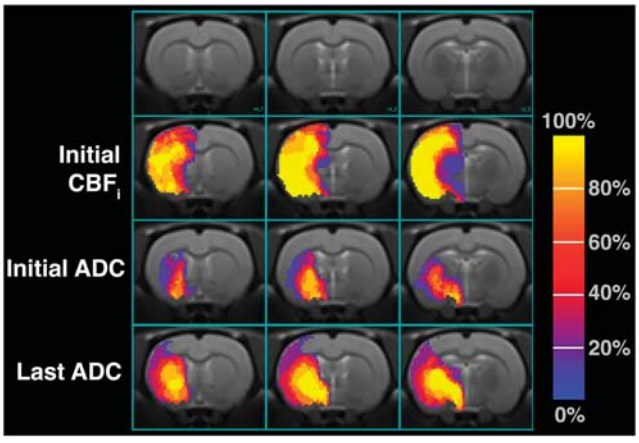

Figure 2 Frequency of initial perfusion, initial (39 ± 6 minutes), and late (237 ± 54 minutes) diffusion lesions across eight rats in three coronal slices corresponding to bregma + 0.7, −1.0, and −1.3 mm in the Paximos-Watson Rat Brain atlas. Voxels with values of 100% mean eight rats had a lesion voxel in that location. Voxels with values of 0% show that none of the eight rats exhibited a lesion at that spatial position. ADC, apparent diffusion coefficient; CBF_i, cerebral blood flow index.

Table 1 ABG measurements obtained at 1.5 hours and 3 hours post-occlusion during RA or NBO and at baseline and at end of MRI (final) studies during RA

	Baseline (24 ± 8 minutes)	*1.5 Hours ABG (98 ± 7 minutes)* N = 8		*3 Hours ABG (177 ± 23 minutes)* N = 6		*Final ABG (251 ± 34 minutes)* N = 7
	RA	*RA*	*NBO*	*RA*	*NBO*	*RA*
pH	7.37 ± 0.03	7.33 ± 0.03[a,f]	7.32 ± 0.03[e,j]	7.34 ± 0.02[g]	7.34 ± 0.02	7.37 ± 0.02
pCO_2 (mm Hg)	34.9 ± 5.6	37.4 ± 5.5	41.3 ± 6.5	38.2 ± 6.1	39.6 ± 4.8	44.1 ± 6.5
pO_2 (mm Hg)	93.6 ± 16.1	88.2 ± 7.7	312 ± 98[d,h,k]	84.1 ± 8.0	355 ± 44[d,h,k]	84.9 ± 16.3
MABP (mm Hg)	99.0 ± 14.2[n]	75.8 ± 11.7[b]	101 ± 12.1[i,l]	79.7 ± 5.8[c]	96.7 ± 11.1[m]	81.8 ± 15.5

ABG, arterial blood gas; MABP, mean arterial blood pressure; MCAO, middle cerebral artery occlusion; MRI, magnetic resonance image; NBO, normobaric oxygen; RA, room air.
Values are shown as mean ± standard deviation. Values in parentheses are the time the ABG was acquired post-MCAO. [a]$P = 0.002$, [b]$P = 0.003$, [c]$P = 0.05$ RA vs. baseline; [d]$P < 0.0001$, [e]$P = 0.04$ NBO vs. baseline; [f]$P = 0.001$, [g]$P = 0.04$ RA vs. final; [h]$P < 0.0001$, [i]$P = 0.008$, [j]$P = 0.02$ NBO vs. final; [k]$P < 0.0001$, [l]$P = 0.001$, [m]$P = 0.04$ NBO vs. RA, [n]$P = 0.01$ baseline vs. final.

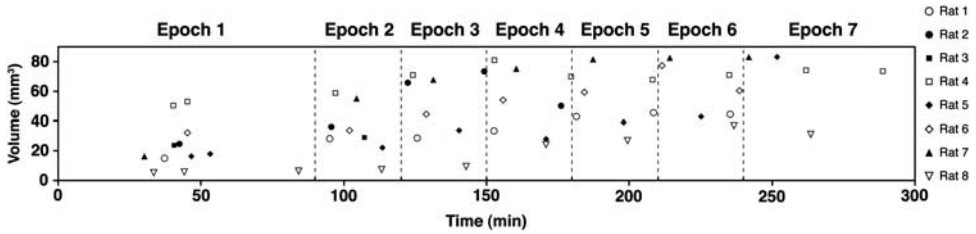

Figure 3 Apparent diffusion coefficient lesion volume changes over time for all rats.

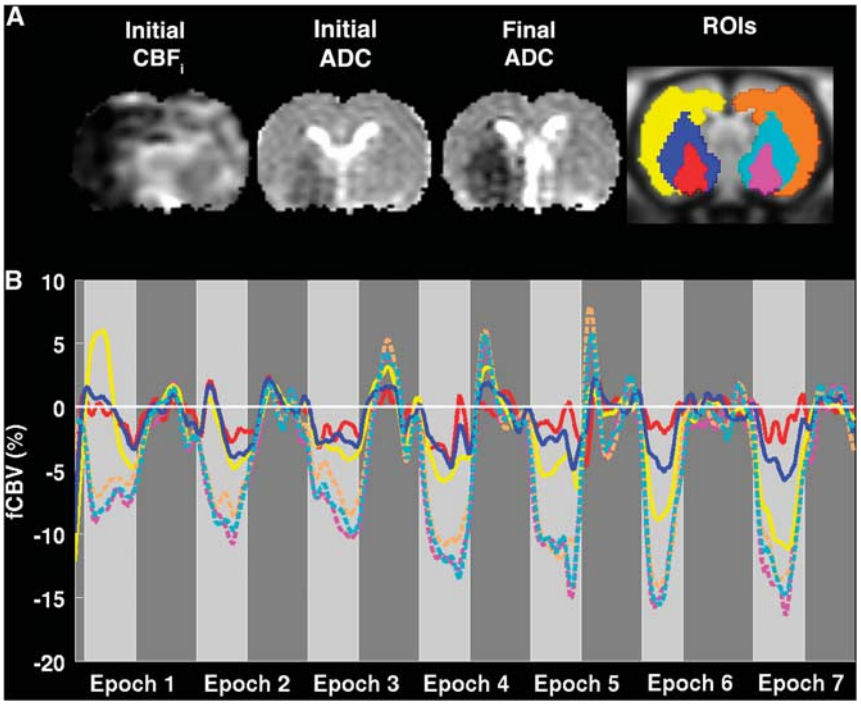

Figure 4 (**A**) Initial cerebral blood flow (CBF) and apparent diffusion coefficient (ADC) and final ADC maps are shown along with Core (red), Growth (blue), and Saved (yellow) regions of interest (ROIs) and mirrored contralateral counterparts (pink, cyan, and orange, respectively) for Rat 1. (**B**) Baseline-corrected smoothed temporal responses in these regions are shown for Core, Growth, Saved (red, blue, and yellow solid lines, respectively), and contralateral regions (pink, cyan, and orange dashed lines, respectively) for Rat 1. Light gray regions represent periods of normobaric oxygen (NBO) and dark gray regions represent exposure to room air. For the Core region, very little change is observed in response to NBO over time. Regions of Saved tissue (yellow) exhibited early vasodilation, which over time demonstrated vasoconstriction. Early on, regions of lesion expansion (blue) demonstrated no significant change in response to NBO, but eventually exhibited some vasoconstriction, but not to the same degree as contralateral (dashed lines) or saved (yellow) tissue. fCBV, functional cerebral blood volume.

and Saved ROIs. Tissue that stayed viable by the end of the experiment (Saved) showed relatively preserved mean fCBV (Figure 5) and some rats (Figure 4) showed statistically significant increases in fCBV (*vasodilation*) in Epoch 1; intermediate epochs showed moderate vasoconstriction; and by 3 hours there was marked vasoconstriction. In comparison, tissue that became ADC abnormal over time (Growth) demonstrated little initial fCBV response to NBO and only exhibited slight vasoconstriction after 3 hours, but not to the same extent as contralateral or Salvaged tissue. These effects were observed for all animals using ROI analysis (Figure 5). Ipsilesional tissue demonstrated significantly smaller decreases in CBV compared with contralesional tissue at all time points. All ROIs, except for the Core, exhibited greater decreases in fCBV, i.e., greater vasoconstriction, over time.

Voxel-based GLM analysis also demonstrated spatially and temporally heterogeneous responses in fCBV (Figure 6). This was especially evident for the first challenge, Epoch 1, for which both increases and decreases in response to NBO were observed (78 ± 7 minutes, Figure 6A), consistent with our ROI analysis results (Figure 5). Figure 6A is a voxel-based representation of which voxels across all animals showed significant differences ($P < 0.0001$) in response to NBO compared with RA within the first 1.5 hours. In the ipsilesional hemisphere, a transient increase of CBV in regions outside of the core but encompassed by the area with perfusion abnormalities

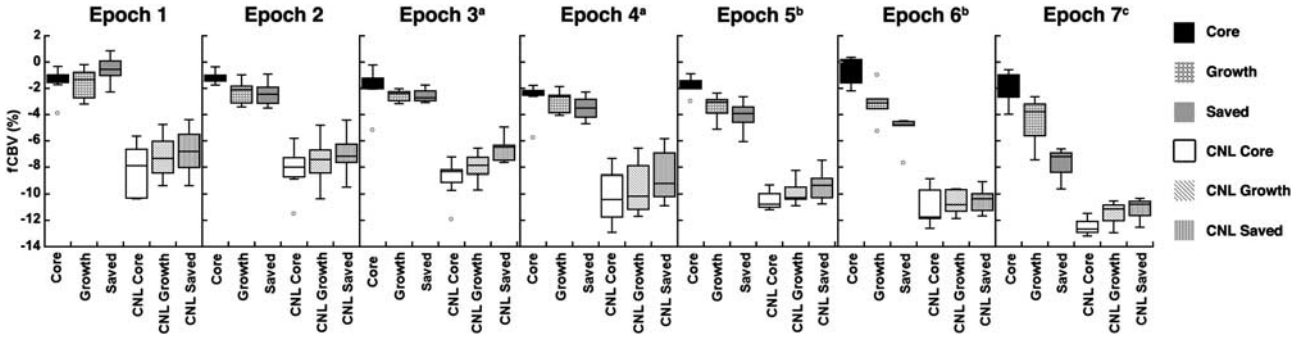

Figure 5 Functional cerebral blood volume (fCBV) changes over time in Core, Growth, Saved, and mirror contralateral (CNL) regions of interest (ROIs) for all animals. Core, Growth, and Saved ROIs exhibited significantly less CBV decreases than their mirror counterparts for all Epochs ($P < 0.006$). The Saved ROI exhibited both increases and decreases during Epoch 1, significantly different compared with Core ($P = 0.02$) and Growth ($P = 0.02$). Both Growth and Saved exhibited greater decreases in CBV than Core during Epoch 2 ($P = 0.003$, $P < 0.001$), Epoch 5 ($P = 0.002$, $P < 0.001$), Epoch 6 ($P < 0.001$, $P < 0.001$), and Epoch 7 ($P = 0.002$, $P < 0.001$). The Saved ROI showed significantly greater CBV decreases than the Growth ROI during Epoch 5 ($P = 0.002$), Epoch 6 ($P < 0.001$), and Epoch 7 ($P < 0.001$). CNL Core CBV changes were significantly less than CNL Growth CBV changes ($P = 0.04$) and CNL Saved CBV changes ($P = 0.002$) during Epoch 1. CNL Saved had significantly less CBV decreases than CNL Core and CNL Growth during Epoch 2 ($P < 0.001$, $P = 0.02$), Epoch 4 ($P = 0.002$, $P = 0.01$), and Epoch 5 ($P = 0.005$, $P = 0.04$). During Epoch 3, all CNL ROIs exhibited significantly different CBV changes. All ROIs except for Core exhibited significant changes as a function of time ($P < 0.01$). [a]$N = 7$, [b]$N = 5$, [c]$N = 3$, otherwise $N = 8$ (B).

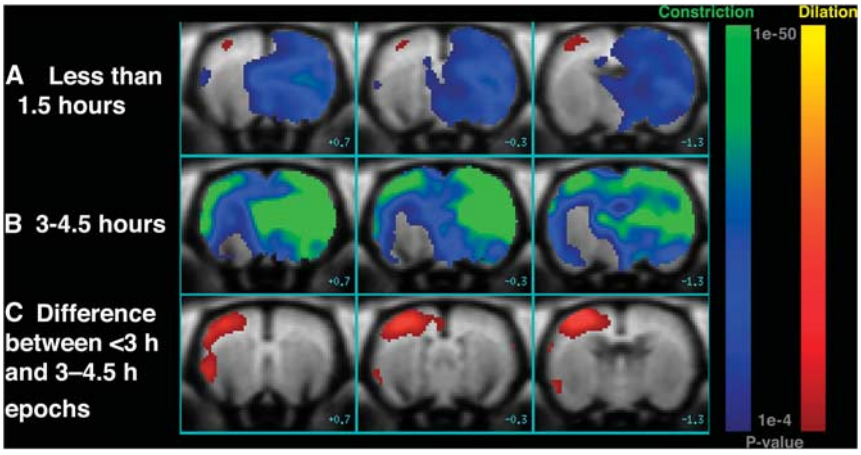

Figure 6 Voxel-based GLM analyses results of functional cerebral blood volume (fCBV) changes in response to normobaric oxygen (NBO) compared with room air for (**A**) Epoch 1 (< 1.5 hours) across eight animals and (**B**) Epochs 5 to 7 (3 to 4.5 hours) across six animals. Areas in red to yellow represent vasodilation, whereas those in green to blue correspond to areas of vasoconstriction (**A**, **B**). (**C**) Difference in NBO responses at < 3 hours compared with NBO responses at 3 to 4.5 hours responses. For **C**, red–yellow regions represent voxels for which NBO-induced fCBV changes were significantly more negative in the late epochs compared with the early epochs, suggesting altered response from early vasodilatation or minimal vasoconstriction to increasingly larger magnitude of vasoconstriction. Color bars show *P* value < 0.0001, where red-to-yellow are positive responses (indicating vasodilation), and blue-to-green are negative responses (representing vasoconstriction).

(i.e., the region of ADC-perfusion 'mismatch') was observed, indicating NBO-induced vasodilatation. In the corresponding contralesional region, we observed significant decreases in CBV, indicating vasoconstriction in response to NBO challenge. It should be noted that the region demonstrating significant vasodilatation (red shading in Figure 6A) is only 3.2 mm^3, compared with mean ADC and CBF_i mismatch (67.3 ± 14.3 mm^3), ~4.8% (Figure 2). Figure 6B is a voxel-based representation of which voxels across all animals 3 to 4.5 hours post-MCAO (Epochs 5 to 7) exhibited significant differences in response to NBO compared with RA. For late challenges (Figures 5 and 6B), increased fCBV responses were no longer evident in the ipsilesional hemisphere, potentially due to microvascular collapse from infarct growth in the Growth ROI and tissue salvage in Saved ROI. The contralateral hemisphere continued to show significant decreases in fCBV in response to NBO. Figure 6C shows the voxel-based differences in fCBV responses to NBO within 3 hours of MCAO (Epochs 1 to 4) and to NBO after 3 hours (Epochs 5–7). The magnitude of fCBV changes appear to be most significant in the Saved ROI region. We did not find a

significant correlation between fCBV and MABP response to NBO (data not shown) suggesting blood pressure changes or increased systemic resistance do not explain the observed fCBV responses.

Discussion

Our study shows that fCBV responses to NBO are spatially and temporally heterogeneous. The contralesional non-ischemic hemisphere showed persistent and potent decreases in CBV with repeated NBO exposures, consistent with the known vasoconstrictive effects of NBO. In the ipsilesional hemisphere, tissue within the acute infarct 'Core' showed no significant CBV response to NBO exposures. In the DWI and PWI 'mismatch' regions of Growth and Saved, ~4.8% tissue regions that remained viable (Saved ROIs) showed significant early increases in CBV (paradoxical vasodilatation), but this response was not sustained; tissue that eventually infarcted (Growth ROIs) showed marginal CBV changes initially and later showed some vasoconstriction. Note that the percentage of tissue showing paradoxical vasodilation is dependent on statistical thresholds; we favored a high statistical threshold ($P < 0.0001$) to ensure the reliability of our results. We speculate that the observed early fCBV responses results from improved tissue viability and neurovascular coupling (Dirnagl, 1997; Shin *et al*, 2006), or shunting of blood from surrounding vasoconstricted tissue ('reverse steal'), or both. These hemodynamic effects likely contribute to the peri-infarct tissue salvage known to occur with early NBO therapy.

The significant increases in fCBV were primarily limited to cortical surfaces (Figure 6), consistent with cortical salvage documented in virtually every NBO experimental stroke study. However, the proportion of tissue showing these increases compared with the entire 'mismatch' region is relatively small. A potential reason for why observed increases were limited to cortical surfaces may be due to the greater proportion of arteries and arterioles in this region that can respond to NBO with greater CBV increases (Zaharchuk *et al*, 1999) than other areas. A second possible explanation is that the first epoch was imaged relatively late (78 ± 7 minutes), i.e., outside NBO's therapeutic time window, and earlier effects of NBO in the entire mismatch region were not captured. A third explanation is that increased perfusion may have occurred within the penumbral areas due to improved flow (Shin *et al*, 2007). Future studies involving serial measurements of both CBF and fCBV in response to NBO challenges using techniques such as continuous assessment of perfusion by tagging, including volume and water extraction (Zaharchuk *et al*, 1998) should be performed to investigate these possibilities.

The evolution of changes in 'mismatch' regions and particularly the differences in temporal responses in Saved and Growth tissue may reflect differences in tissue viability, late autoregulation failure, and eventual microvascular collapse. Autoregulatory vasodilation has been shown to lead to increased CBV in tissue in response to reduced cerebral perfusion pressure as a result of ischemia. However, if the capacity for compensatory vasodilation is exceeded, autoregulation will fail causing tissue dysfunction (Powers, 1991), drop in CBV (Zaharchuk *et al*, 1999), and ultimately death. We speculate that as ischemia persists over time, autoregulation in peri-infarct tissue fails, resulting in inability to vasodilate in response to oxygen, as in the case of tissue within the Growth ROI. This loss of autoregulation in conditions of continued ischemia has been shown for hypercapnic challenges and hypotension induced by blood withdrawal (Zaharchuk *et al*, 1999). However, for tissue in the Saved ROI, repeated NBO challenges may have supported this tissue, allowing for normalized hemodynamic responses over time. Another possibility may be that in early phases, NBO rescues vascular function, protects against microvascular collapse, and thereby salvages tissue. Therefore, NBO's key therapeutic contribution may be for extending the therapeutic time window in acute stroke patients by temporarily raising peri-lesional blood flow delivery. It might be an ideal bridging therapy that can be given in the ambulance before hospital arrival. Patients given NBO can then be further screened for extended time window thrombolytic therapy particularly if they exhibit a target DWI and PWI mismatch pattern (Albers *et al*, 2006).

The presence of 'mismatch' between DWI lesions, assumed to represent the infarct core, and a larger hypoperfused region on bolus-tracking PWI, has been proposed to be a surrogate for salvageable brain tissue to drive clinical decision making for stroke thrombolysis. However, the merits of this technique are still debated as a result of some studies showing that DWI lesions are potentially reversible (Kidwell *et al*, 2000), and may comprise regions that may fulfill the PET criteria for potentially salvageable tissue (Guadagno *et al*, 2006). Moreover, there is ambiguity about the optimal perfusion threshold that can distinguish benign oligemia from 'penumbral' tissue (Dani *et al*, 2011). Clinical trials using 'mismatch' as a selection criteria for thrombolysis have shown variable success (Davis *et al*, 2008; Hacke *et al*, 2005, 2009). An imaging marker of stunned but potentially salvageable tissue may help to overcome shortcomings of DWI and PWI. Recent studies, based on early animal experiments documenting BOLD signal changes in response to oxygen challenge (Kennan *et al*, 1997; Kwong *et al*, 1995), have attempted to use T2*-weighted imaging as a means to more accurately delineate the penumbra (Geisler *et al*, 2006). Under normal conditions, the difference in T2*-weighted signal between ischemic and non-ischemic brain is shown to exist but inadequate to be of clinical utility. Over the last few years, investigators from Glasgow University have shown

that brief periods of NBO exposure ('hyperoxia challenge'), by amplifying the change in oxyhemoglobin/deoxyhemoglobin ratios and T2*-weighted signal, can be used to distinguish potentially viable tissue within hypoperfused brain regions in rodent stroke models and in stroke patients (Dani *et al*, 2010; Robertson *et al*, 2011; Santosh *et al*, 2008). However, T2*-weighted signal changes can be difficult to interpret due to the interplay between NBO-induced changes in arterial oxygenation, CBF, CBV, and even cellular metabolism (Corfield *et al*, 2001; Lu *et al*, 2009). Our study isolated the role of CBV in this process by using a superparamagnetic intravascular MRI contrast agent with long blood half-life (MION). We used short echo times to minimize BOLD contributions. Furthermore, pCO_2, which can also affect CBV, was maintained within the normal range. We also found significant increases in MABP during NBO, which are consistent with results from a previous study in normal human volunteers that showed significant increases in both systemic resistance and brachial blood pressure (Daly and Bondurant, 1962). Changes in MABP were incorporated into the GLM model to account for this potential confound. We speculate that for stroke patients imaged in the hyperacute setting, i.e., within 1.5 hours of stroke onset, vasodilation will be observed, resulting in reduced T2*-weighted imaging values. Furthermore, our findings within 4.5 hours of stroke suggest that potentially salvageable tissue will demonstrate greater vasoconstriction than irreversibly injured tissue. In turn, this will translate to greater increases on T2*-weighted imaging values in this region. In fact this was observed in a study in human stroke patients imaged within 8 hours of onset (Dani *et al*, 2010). Our results therefore extend prior work by showing that NBO-induced hemodynamic changes can also serve as a non-invasive marker for identifying potentially salvageable tissue following stroke.

It is important to note that as in previous studies using this block design, the duration of NBO exposures was limited to a few minutes. The temporal CBV changes observed in our study may not reflect the effects of 'therapeutic' NBO (continuous high-flow oxygen delivery for several hours). The block design was used to investigate the temporal evolution of NBO exposures; we predict that continuous NBO will result in greater neuroprotection with more robust and sustained CBV changes. Furthermore, in-bore occlusion with earlier initiation of NBO (i.e., within its therapeutic time window of 30 to 45 minutes; Singhal *et al*, (2002)) may show more profound CBV responses. As our study focused on investigating hemodynamic changes, we did not assess tissue salvage using histopathologic or functional neurologic outcomes. A limitation of our study is the relatively small number of animals. However, this is offset by use of prolonged multimodal imaging and advanced statistical analysis with very low P value thresholds and a minimum cluster size of 5 voxels, in order to minimize false-positive results in our voxel-based analyses. Future studies should investigate whether lower concentrations of NBO result in equivalent CBV responses with limited influence on CBF and MABP, as has been shown for the overall T2* effect (Baskerville *et al*, 2011).

In summary, our results show that NBO induces heterogenous CBV changes that appear to reflect the hemodynamic status of brain tissue after stroke, and that NBO challenge may be a useful imaging technique to distinguish salvageable from non-salvageable tissue. Clinical translation may advance the field of acute stroke imaging and improve therapeutic decision making for thrombolysis and other neuroprotective strategies.

Acknowledgements

We thank Dr Ralph Weissleder and Ms Tina Balducci of the Center for Molecular Imaging Research at the Massachusetts General Hospital for synthesizing and distributing the MION contrast agent used in this study.

Disclosure/conflict of interest

The authors declare no conflict of interest.

References

Albers GW, Thijs VN, Wechsler L, Kemp S, Schlaug G, Skalabrin E, Bammer R, Kakuda W, Lansberg MG, Shuaib A, Coplin W, Hamilton S, Moseley M, Marks MP (2006) Magnetic resonance imaging profiles predict clinical response to early reperfusion: the diffusion and perfusion imaging evaluation for understanding stroke evolution (DEFUSE) study. *Ann Neurol* 60:508–17

Baskerville TA, Deuchar GA, McCabe C, Robertson CA, Holmes WM, Santosh C, Macrae IM (2011) Influence of 100% and 40% oxygen on penumbral blood flow, oxygen level, and T2*-weighted MRI in a rat stroke model. *J Cereb Blood Flow Metab* 31:1799–806

Corfield DR, Murphy K, Josephs O, Adams L, Turner R (2001) Does hypercapnia-induced cerebral vasodilation modulate the hemodynamic response to neural activation? *NeuroImage* 13:1207–11

Cox RW (1996) AFNI: software for analysis and visualization of functional magnetic resonance neuroimages. *Computers Biomed. Res.* 29:162–73

Daly WJ, Bondurant S (1962) Effects of oxygen breathing on the heart rate, blood pressure, and cardiac index of normal men—resting, with reactive hyperemia, and after atropine. *J Clin Invest* 41:126–32

Dani KA, Santosh C, Brennan D, McCabe C, Holmes WM, Condon B, Hadley DM, Macrae IM, Shaw M, Muir KW (2010) T2*-weighted magnetic resonance imaging with hyperoxia in acute ischemic stroke. *Ann Neurol* 68:37–47

Dani KA, Thomas RG, Chappell FM, Shuler K, MacLeod MJ, Muir KW, Wardlaw JM (2011) Computed tomography and magnetic resonance perfusion imaging in ischemic stroke: definitions and thresholds. *Ann Neurol* 70:384–401

Davis SM, Donnan GA, Parsons MW, Levi C, Butcher KS, Peeters A, Barber PA, Bladin C, De Silva DA, Byrnes G, Chalk JB, Fink JN, Kimber TE, Schultz D, Hand PJ, Frayne J, Hankey G, Muir K, Gerraty R, Tress BM, Desmond PM (2008) Effects of alteplase beyond 3 hours after stroke in the Echoplanar Imaging Thrombolytic Evaluation Trial (EPITHET): a placebo-controlled randomised trial. *Lancet Neurol* 7:299–309

Dirnagl U (1997) Metabolic aspects of neurovascular coupling. *Adv Exp Med Biol* 413:155–9

Geisler BS, Brandhoff F, Fiehler J, Saager C, Speck O, Rother J, Zeumer H, Kucinski T (2006) Blood-oxygen-level-dependent MRI allows metabolic description of tissue at risk in acute stroke patients. *Stroke* 37:1778–84

Guadagno JV, Warburton EA, Jones PS, Day DJ, Aigbirhio FI, Fryer TD, Harding S, Price CJ, Green HA, Barret O, Gillard JH, Baron JC (2006) How affected is oxygen metabolism in DWI lesions?: A combined acute stroke PET-MR study. *Neurology* 67:824–9

Hacke W, Albers G, Al-Rawi Y, Bogousslavsky J, Davalos A, Eliasziw M, Fischer M, Furlan A, Kaste M, Lees KR, Soehngen M, Warach S (2005) The Desmoteplase in Acute Ischemic Stroke Trial (DIAS): a phase II MRI-based 9-hour window acute stroke thrombolysis trial with intravenous desmoteplase. *Stroke* 36:66–73

Hacke W, Furlan AJ, Al-Rawi Y, Davalos A, Fiebach JB, Gruber F, Kaste M, Lipka LJ, Pedraza S, Ringleb PA, Rowley HA, Schneider D, Schwamm LH, Leal JS, Sohngen M, Teal PA, Wilhelm-Ogunbiyi K, Wintermark M, Warach S (2009) Intravenous desmoteplase in patients with acute ischaemic stroke selected by MRI perfusion-diffusion weighted imaging or perfusion CT (DIAS-2): a prospective, randomised, double-blind, placebo-controlled study. *Lancet Neurol* 8:141–50

Henninger N, Bouley J, Nelligan JM, Sicard KM, Fisher M (2007) Normobaric hyperoxia delays perfusion/diffusion mismatch evolution, reduces infarct volume, and differentially affects neuronal cell death pathways after suture middle cerebral artery occlusion in rats. *J Cereb Blood Flow Metab* 27:1632–42

Hoehn-Berlage M, Norris DG, Kohno K, Mies G, Leibfritz D, Hossmann KA (1995) Evolution of regional changes in apparent diffusion coefficient during focal ischemia of rat brain: the relationship of quantitative diffusion NMR imaging to reduction in cerebral blood flow and metabolic disturbances. *J Cereb Blood Flow Metab* 15:1002–11

Kennan RP, Scanley BE, Gore JC (1997) Physiologic basis for BOLD MR signal changes due to hypoxia/hyperoxia: separation of blood volume and magnetic susceptibility effects. *Magn Reson Med* 37:953–6

Kidwell CS, Saver JL, Mattiello J, Starkman S, Vinuela F, Duckwiler G, Gobin YP, Jahan R, Vespa P, Kalafut M, Alger JR (2000) Thrombolytic reversal of acute human cerebral ischemic injury shown by diffusion/perfusion magnetic resonance imaging. *Ann Neurol* 47:462–9

Kwong KK, Donahue KM, Ostergaard L, Shen T, Bandettini PA, Wanke I, Moore J, Rosen BR (1995) Mechanism of MR brain signal increase in hyperoxia. In *Proceedings of SMRM 3rd Annual Meeting*. Nice, France, pp 768

Lassen NA, Palvolgyi R (1968) Cerebral steal during hypercapnia and the inverse reaction during hypocapnia observed by the 133 xenon technique in man. *Scand J Clin Lab Invest Suppl* 102:XIII:D

Liu CH, Greve DN, Dai G, Marota JJ, Mandeville JB (2007) Remifentanil administration reveals biphasic phMRI temporal responses in rat consistent with dynamic receptor regulation. *NeuroImage* 34:1042–53

Liu S, Liu W, Ding W, Miyake M, Rosenberg GA, Liu KJ (2006) Electron paramagnetic resonance-guided normobaric hyperoxia treatment protects the brain by maintaining penumbral oxygenation in a rat model of transient focal cerebral ischemia. *J Cereb Blood Flow Metab* 26:1274–84

Lodato RF (1989) Decreased O2 consumption and cardiac output during normobaric hyperoxia in conscious dogs. *J Appl Physiol* 67:1551–9

Longa EZ, Weinstein PR, Carlson S, Cummins R (1989) Reversible middle cerebral artery occlusion without craniectomy in rats. *Stroke* 20:84–91

Lu J, Dai G, Egi Y, Huang S, Kwon SJ, Lo EH, Kim YR (2009) Characterization of cerebrovascular responses to hyperoxia and hypercapnia using MRI in rat. *NeuroImage* 45:1126–34

Mandeville JB, Jenkins BG, Chen YC, Choi JK, Kim YR, Belen D, Liu C, Kosofsky BE, Marota JJ (2004) Exogenous contrast agent improves sensitivity of gradient-echo functional magnetic resonance imaging at 9.4 T. *Mag Reso Med* 52:1272–81

Mandeville JB, Marota JJ, Kosofsky BE, Keltner JR, Weissleder R, Rosen BR, Weisskoff RM (1998) Dynamic functional imaging of relative cerebral blood volume during rat forepaw stimulation. *Mag Reson Med* 39: 615–24

Miyabe M, Mori S, van Zijl PC, Kirsch JR, Eleff SM, Koehler RC, Traystman RJ (1996) Correlation of the average water diffusion constant with cerebral blood flow and ischemic damage after transient middle cerebral artery occlusion in cats. *J Cereb Blood Flow Metab* 16:881–91

Nakajima S, Meyer JS, Amano T, Shaw T, Okabe T, Mortel KF (1983) Cerebral vasomotor responsiveness during 100% oxygen inhalation in cerebral ischemia. *Arch Neurol* 40:271–6

Powers WJ (1991) Cerebral hemodynamics in ischemic cerebrovascular disease. *Ann Neurol* 29:231–40

Robertson CA, McCabe C, Gallagher L, Lopez-Gonzalez Mdel R, Holmes WM, Condon B, Muir KW, Santosh C, Macrae IM (2011) Stroke penumbra defined by an MRI-based oxygen challenge technique: 1. Validation using [14C]2-deoxyglucose autoradiography. *J Cereb Blood Flow Metab* 31:1778–87

Santosh C, Brennan D, McCabe C, Macrae IM, Holmes WM, Graham DI, Gallagher L, Condon B, Hadley DM, Muir KW, Gsell W (2008) Potential use of oxygen as a metabolic biosensor in combination with T2*-weighted MRI to define the ischemic penumbra. *J Cereb Blood Flow Metab* 28:1742–53

Shin HK, Dunn AK, Jones PB, Boas DA, Lo EH, Moskowitz MA, Ayata C (2007) Normobaric hyperoxia improves cerebral blood flow and oxygenation, and inhibits peri-infarct depolarizations in experimental focal ischaemia. *Brain* 130:1631–42

Shin HK, Dunn AK, Jones PB, Boas DA, Moskowitz MA, Ayata C (2006) Vasoconstrictive neurovascular coupling during focal ischemic depolarizations. *J Cereb Blood Flow Metab* 26:1018–30

Singhal AB (2007) A review of oxygen therapy in ischemic stroke. *Neurol Res* 29:173–83

Singhal AB, Benner T, Roccatagliata L, Koroshetz WJ, Schaefer PW, Lo EH, Buonanno FS, Gonzalez RG, Sorensen AG (2005) A pilot study of normobaric oxygen therapy in acute ischemic stroke. *Stroke* 36:797–802

Singhal AB, Dijkhuizen RM, Rosen BR, Lo EH (2002) Normobaric hyperoxia reduces MRI diffusion abnorm-

alities and infarct size in experimental stroke. *Neurology* 58:945–52

Singhal AB, Ratai E, Benner T, Vangel M, Lee V, Koroshetz WJ, Schaefer PW, Sorensen AG, Gonzalez RG (2007) Magnetic resonance spectroscopy study of oxygen therapy in ischemic stroke. *Stroke* 38:2851–4

Sorensen AG, Wu O, Copen WA, Davis TL, Gonzalez RG, Koroshetz WJ, Reese TG, Rosen BR, Wedeen VJ, Weisskoff RM (1999) Human acute cerebral ischemia: detection of changes in water diffusion anisotropy by using MR imaging. *Radiology* 212:785–92

Worsley KJ, Liao CH, Aston J, Petre V, Duncan GH, Morales F, Evans AC (2002) A general statistical analysis for fMRI data. *NeuroImage* 15:1–15

Zaharchuk G, Bogdanov AA, Jr, Marota JJ, Shimizu-Sasamata M, Weisskoff RM, Kwong KK, Jenkins BG, Weissleder R, Rosen BR (1998) Continuous assessment of perfusion by tagging including volume and water extraction (CAPTIVE): a steady-state contrast agent technique for measuring blood flow, relative blood volume fraction, and the water extraction fraction. *Mag Reson Med* 40:666–78

Zaharchuk G, Mandeville JB, Bogdanov AA, Jr, Weissleder R, Rosen BR, Marota JJ (1999) Cerebrovascular dynamics of autoregulation and hypoperfusion. An MRI study of CBF and changes in total and microvascular cerebral blood volume during hemorrhagic hypotension. *Stroke* 30:2197–204